Nature Environment and Pollution Technology
An International Quarterly Scientific Journal

p-ISSN: 0972-6268
(Print copies up to 2016)
e-ISSN: 2395-3454

Vol. 19 | No. 2 | pp. 889-895 | 2020

Original Research Paper

https://doi.org/10.46488/NEPT.2020.v19i02.049

Open Access Journal

Facile Preparation of β-Fe_2O_3/$BiOCl_{0.875}Br_{0.125}$ Composites for Enhanced Visible-light Photocatalytic Degradation of Organics from Water

Jihao Zhou*, Zhiwei Zhao, Ping Xiao***, Jie Liu*, Zhaoxia Ding*†, Yuting Han*** and Jie Shi******

*Department of Military Facilities, Army Logistics University, Chongqing, 401331, China
**College of Environment and Ecology, Chongqing University, Chongqing, 400044, China
***Green Intelligence Environmental School, Yangtze Normal University, Chongqing 408100, China
****PLA, No. 93413, Yongji, Shanxi 044500, China
†Corresponding author: Zhaoxia Ding (E-mail: Jihao Zhou; rainbowin@qq.com)

Nat. Env. & Poll. Tech.
Website: www.neptjournal.com

Received: 30-06-2019
Accepted: 30-08-2019

Key Words:
Bismuth oxyhalide;
Catalyst modification;
Organics degradation;
Visible-light photocatalysis

ABSTRACT

Visible light-driven photocatalytic oxidation technology has shown great potential for effective removal of organic pollutants from water and mitigation of energy crises at the same time. The highly effective and economic β-Fe_2O_3/$BiOCl_{0.875}Br_{0.125}$ photocatalyst was prepared by a facile hybrid compositing method with β-Fe_2O_3 and $BiOCl_{0.875}Br_{0.125}$ to overcome relatively high material cost and limited catalytic efficiency. Characterization techniques, such as XRD, SEM and XPS were used to study the purity and crystallization characteristics of the as-prepared photocatalyst. Furthermore, taking rhodamine b (RhB) as a simulated organic pollutant, the photocatalytic property of β-Fe_2O_3/$BiOCl_{0.875}Br_{0.125}$ with different Bi content was further evaluated by static catalytic degradation test under visible-light. The results indicated that the photocatalytic efficiency of the novel composites increases with the improvement of Bi content. Additionally, in comparison to equal mass of pure phase $BiOCl_{0.875}Br_{0.125}$, when the Bi content reached to 30%, a comparable and even better photocatalysis performance was achieved by the as-prepared β-Fe_2O_3/$BiOCl_{0.875}Br_{0.125}$. The hybrid β-Fe_2O_3/$BiOCl_{0.875}Br_{0.125}$ has a potential cost advantage in practical water treatment, and provide an attractive method for fabricating efficient visible-light-driven photocatalysts.

INTRODUCTION

In the past decades, with the rapid development of modern industry and agriculture, environmental and energy-related issues are increasingly becoming two major problems facing humanity (Elimelech & Phillip 2011). A wide range of pollution sources including domestic sewage, pesticides, pharmaceuticals, and chemicals, have aggressively spread around the soil, atmosphere, and the natural waters, resulting in serious damage to the ecosystem (Omenn 2006). Water safety, as one of the current high-profile topics, is seriously threatened by various Persistent Organic Pollutants (POPs) (Zhang et al. 2019). Therefore, seeking efficacious technologies for the removal of POPs is of particular importance to ensure safe production of drinking water and sustainable development of aquatic environment. At present, traditional methods for treating organic pollutants in water mainly include biological treatment, chemical oxidation, membrane filtration and adsorption (Hasan & Jhung 2015). However, there are always some inevitable defects hidden behind these conventional processes, such as the inability to completely degrade organic pollutants, high cost, and the easiness to produce secondary pollution, and so on (Amini et al. 2015). Advanced oxidation processes (AOPs)-based treatment technologies are receiving special recognition as alternatives to traditional water disposal processes and as a means of effluent polishing for water reclamation (Ribeiro et al. 2015, Deng & Zhao 2015). Since the AOPs have been continuously proven to perform a significant effect on the removal of organic pollutants with high stability and toxicity in water, exploring novel AOPs with strong degradation efficiency, low cost, high stability, mild reaction conditions and no secondary pollution, occupied the position of the hottest research field currently.

Photocatalytic oxidation technology is one of the most promising AOPs and growing popularity to be applied to water treatment due to its unique advantages like highly efficient organic mineralization, energy-saving, non-toxic, and no or fewer chemicals consume. Photocatalysis is inseparable from photocatalysts. By utilizing the energy of light to convert into the chemical energy required for chemical reactions, photocatalysts can degrade almost all harmful organic pollutants and some inorganic substances, accelerating

chemical reactions (Hoffmann et al. 1995). It recognized that once the semiconductor photocatalyst was subjected to light illumination (visible or ultraviolet light), the electrons on the valence band are excited to leap into the conduction band, resulting in leaving behind a hole in the valence band (Lee et al. 2016, Masih et al. 2017, Martin et al. 2015). Thus, the hole-electron pairs are continually generated in the presence of the electrostatic field force. During this process, part of the excited photogenerated electrons and holes migrate to the surface of the photocatalyst, producing multiple strong oxidizing species that are competent to degrade organic contaminants from the water (Jaiswal et al. 2016, Mohamed et al. 2016). Unfortunately, not all photogenerated electron-hole pairs migrate to the semiconductor surface, some of which will recombine in the form of photons. The existence time of the electron-hole pair is very short, but their recombination can still occur inside the photocatalyst, and the recombination rate is the key factor determining the performance of the photocatalyst.

As a new type of photocatalytic material, bismuth oxyhalide (BiOX, X=Cl, Br, I) performs an exceptional photocatalytic activity due to its peculiar layered structure in which X (X=Cl, Br, I) ion layer and $[Bi_2O_2]^{2+}$ layer is alternately arranged. Although BiOX has many advantages, they are still limited in practical applications. To be specific, among the three BiOX, only BiOBr and BiOI possess the narrow enough energy gap with the value of 2.6 and 1.8 eV, respectively, which can be excited by visible light, while BiOCl with an energy gap of 3.2 eV is only allowed to be excited by ultraviolet light (Ren et al. 2013). Besides, in addition to the inferior stability of pure BiOI, the recombination rate of photogenerated electron-hole pairs of three kinds of BiOX in practical applications is relatively fast, resulting in unsatisfactory photocatalytic performance (Li et al. 2014). Thus, aiming to enhance the photocatalytic activity, physical-chemistry stability, photocatalytic response to visible light, as well as to reduce the recombination rate of electron-hole pairs, many attempts such as morphological regulation, complex hybridization and crystal structure control have been carried out to modify BiOX (Ren et al. 2013, Deng et al. 2005, Xiao et al. 2012). However, these modification strategies may be constrained by problems such as complex manufacturing processes or high material costs.

In nature, nano-iron oxide exists mainly in the form of Fe_2O_3 with three crystal configurations of α, β and γ (Brázda et al. 2014). Compared with other metal oxide-based photocatalytic materials, nano-iron oxide, especially in the presence of β-Fe_2O_3, exhibits high structural stability, wide distribution, low preparation cost, and no pollution. Most notable is that the narrow enough bandgap endows β-Fe_2O_3 with excellent visible light absorption performance, which holds great promise in photocatalysis field (Christoforidis et al. 2016). Currently, Br-based blending modification has proven to be an effective way to reduce the electron-hole pair recombination rate of BiOCl (Gnayem & Sasson 2013). However, this method is limited by the large consumption of Bi, which leads to an increase in cost, and there is still room for improvement in the activity of the $BiOCl_xBr_{1-x}$ composite. To the best of our knowledge, from the perspective of composite hybridization, the modification strategy of preparing bismuth oxyhalide-based composite by further compounding β-Fe_2O_3 has not been reported.

The overall objectives of this study were: (1) to successfully synthesize and characterize the hybrid β-Fe_2O_3/$BiOCl_xBr_{1-x}$ composite photocatalyst; (2) to evaluate the photocatalytic degradation performance of β-Fe_2O_3/$BiOCl_xBr_{1-x}$ on organics removal; (3) to analyse the photocatalytic mechanism of the composite material of β-Fe_2O_3/$BiOCl_xBr_{1-x}$.

MATERIALS AND METHODS

Materials: All chemical reagents were of analytical grade and were used as received. Ferric sulphate, sodium sulphate decahydrate, sodium chloride, potassium bromide and rhodamine B (RhB) were purchased from Macklin Biochemical Co., Ltd (China). Other reagents including bismuth nitrate pentahydrate, cetyltrimethylammonium chloride (CTAC), nitric acid and absolute ethyl alcohol were obtained from Sinopharm (China).

Preparation of β-Fe_2O_3, $BiOCl_{0.875}Br_{0.125}$ and β-Fe_2O_3/$BiOCl_{0.875}Br_{0.125}$: Deionized water (15 mL), ferric sulphate (15 mmol), and sodium sulphate decahydrate (15 mmol) are placed into a 50 mL flask followed by stirring and drying at 70°C. The obtained powder products were mixed with 30 mmol of NaCl and ground, and then transferred to a tube furnace (SKGL-1200M, SIOMM, China) and calcinated at 500°C for 1 h.

For the synthesis of $BiOCl_xBr_{1-x}$, according to the method reported by Gnayem & Sasson (2013), the procedure of preparing a 3D flower-like $BiOCl_{0.875}Br_{0.125}$ with relatively high photocatalysis activity are as follows: Deionized water (50 mL) and bismuth nitrate pentahydrate (5 mmol) are mixed in a 150 mL flask and stirred at room temperature for 30 min, the obtained solution was denoted as solution A. Then CTAC (1.36 g dissolved in 25 mL of water,) and potassium bromide (0.09 g, 0.75 mmol) are added to the above solution in one batch, following, the obtained flocculent precipitate was magnetically stirred at room temperature for 2 h. The precipitate after centrifugation was washed 3 times with ethanol and deionized water, respectively. The white solid powder

was finally dried at 60 °C in an electrothermal blowing dry box (DHG-9123A, MARIT, China) and was denoted as M0.

For the preparation of β-Fe_2O_3/$BiOCl_{0.875}Br_{0.125}$, a certain amount of β-Fe_2O_3 was added to 40 mL of deionized water, which was subjected to ultrasonic dispersion for 5 min. Afterwards, a certain amount of CTAC and potassium bromide was added to above solution and stirred for 10 min followed by adding different volumes of solution A. After stirring for 2 h, the sample was centrifuged and washed three times with absolute ethanol and deionized water, respectively, and finally dried at 60°C for 6 h. For comparison, a series of β-Fe_2O_3/$BiOCl_{0.875}Br_{0.125}$ with various Bi contents ranging from 10% to 30% were synthesized and the details are presented in Table 1.

Characterization: Employing a scanning electron microscope (SEM, FEI Nova 400 Nano, Philips, Netherlands) to study the morphologies of as-prepared β-Fe_2O_3/$BiOCl_{0.875}Br_{0.125}$. X-ray diffraction (XRD, XRD-6100 Lab, SHIMADZU, Japan) was performed to determine the crystal structure of β-Fe_2O_3/$BiOCl_{0.875}Br_{0.125}$, and its patterns from 20° to 80° were recorded at room temperature following the reported conditions (Gnayem & Sasson 2013). The X-ray photoelectron spectroscopy (XPS, Escalab 250Xi, ThermoFisher Scientific, USA) was carried out to analyse the chemical composition of β-Fe_2O_3/$BiOCl_{0.875}Br_{0.125}$.

Evaluation of photocatalytic property: The RhB, a typical carcinogenic substance from the effluent of the textile industry, was selected as the target organic pollutant to evaluate the photocatalytic performance of as-prepared β-Fe_2O_3/$BiOCl_{0.875}Br_{0.125}$. A 300 W Xe lamp was employed as the visible-light source device (λ> 420 nm, KJS-300W, Kajing Intelligence, China) to simulate natural sunlight. 10 mg of the photocatalyst was added in 50 mL of RhB aqueous solution (20 mg/L). 4 mL of sample was collected at 5, 10, 15, 30 min and filtrated through a 0.22 μm aqueous filter, then was measured at 550 nm with a UV-vis spectrophotometer (DR600, HACH, USA). The degradation rate (D) of RhB was calculated by Eq. (1), and the quasi-first-order kinetic model of this photocatalytic process was shown in Eq. (2).

$$D = [(A_0 - A)/A_0] \times 100\% \quad \ldots(1)$$

$$\ln(A_0/A) = kt \quad \ldots(2)$$

Table 1: β-Fe_2O_3/$BiOCl_{0.875}Br_{0.125}$ prepared with different Bi contents.

name	Bi Content (wt%)	Chemical Addition			
		β-Fe2O3 (g)	CTAC (g)	KBr (g)	Solution A (mL)
M1	10	0.54	0.06	0.004	2
M2	20	0.48	0.12	0.008	4
M3	25	0.45	0.15	0.010	5
M4	30	0.42	0.18	0.012	6

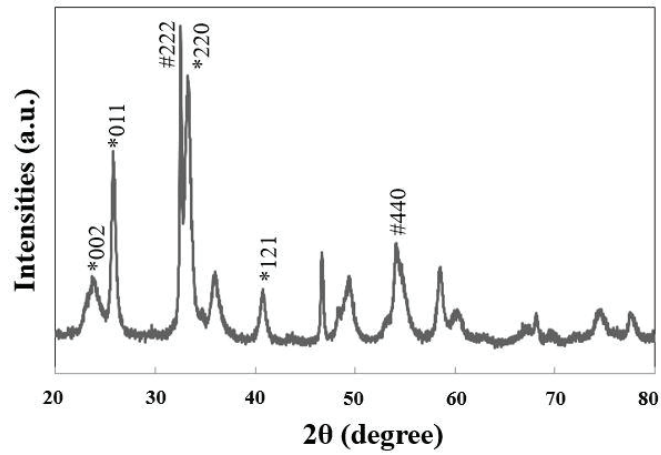

Fig. 1 XRD diffraction pattern of β-Fe_2O_3/$BiOCl_{0.875}Br_{0.125}$

Where, A_0 and A mean the absorbance of RhB solution at 0 and t min under visible-light irradiation, respectively.

RESULTS AND DISCUSSION

Characterization of β-Fe_2O_3/$BiOCl_{0.875}Br_{0.125}$: Fig. 1 displays the XRD diffraction pattern of the composite β-Fe_2O_3/$BiOCl_{0.875}Br_{0.125}$ with a Bi content of 30%. It can be seen that the characteristic diffraction peak of as-prepared β-Fe_2O_3/$BiOCl_{0.875}Br_{0.12}$ coincided with the standard card of the tetragonal BiOX catalyst. Among them, there were strong diffraction peaks at 23.98° and 26.12° corresponding to the diffraction peaks of the (002) and (011) crystal faces of BiOCl. Besides, the peaks at 40.85° and 33.6° were corresponding to the diffraction peaks of the (121) and (220) crystal faces of BiOBr, and these diffraction peaks attributed to BiOX were marked as *. Meanwhile, there are also strong diffraction peaks at 32.7° and 55.21°, which were corresponding to the diffraction peaks of the (222) and (440) crystal faces of β-Fe_2O_3, and were marked as #. As seen in Fig. 1, the intensity of these diffraction peaks were relatively high and the peak shape was sharp, indicating that the composite material synthesized under this condition possessed a superior purity and crystallinity.

Fig. 2 shows the SEM images of the as-prepared β-Fe_2O_3/$BiOCl_{0.875}Br_{0.125}$ sample with a Bi content of 30%. It can be seen from the SEM images at low magnification (a) and high magnification (b) that the synthesized photocatalyst sample had a uniform morphology and size, meanwhile, it exhibited a transparent sheet structure. Fig. 3 indicates the XPS patterns of the composite sample. It can be found from Fig. 3a that the sample had the absorption peaks corresponding to the elements of Bi, Cl, Fe, Br and O, and no absorption peaks of other elements. Besides, the binding energies of the Bi, Cl, Fe and Br elements were attributed to the absorption peaks of Bi 4f, Cl 2p, Fe 2p and Br 3d, respectively (Fig. 3b-3d). From the numerical values of the binding energy of the respective elements, it can be further concluded that the prepared sample had no obvious impurities and exhibited high purity.

Evaluation of the photocatalysis performance: To study the effect of β-Fe_2O_3 doping on the catalytic performance of BiOX, the static photodegradation of RhB over different β-Fe_2O_3/$BiOCl_{0.875}Br_{0.125}$ (10wt%, 20wt%, 25% and 30% of Bi contents) as well as the pure $BiOCl_{0.875}Br_{0.125}$ were shown in Fig. 4. The M1 and M2 present the similarly low degradation efficiency with C/Co of 0.441 and 0.092 after reacting for 30 min, respectively, suggesting that the effective active site exposed to visible light in a short time was incompetent at low Bi contents. However, when the Bi content exceeded 25%, the modified BiOX-based photocatalyst exhibited significantly enhanced degradation efficiency as that the degradation rate of RhB within 15 minutes reached 95.2% and 99.4%, respectively (Fig. 4c and 4d). In comparison to the pure phase $BiOCl_{0.875}Br_{0.125}$ (Fig. 4e), β-Fe_2O_3/$BiOCl_{0.875}Br_{0.125}$ with a Bi content of 30% achieved an excellent photodegradation performance that could be comparable or even better.

In the insets of Fig. 4, the quasi-first-order dynamic models corresponding to each process were also presented, and the coefficients of determination were 0.9629, 0.9547, 0.9939, 0.9638 and 0.9632 in turn, indicating that the model equation could fit the experimental observations well. Besides, the more intuitive comparison of the K value of each reaction is shown in Fig. 5. It can be found that $BiOCl_{0.875}Br_{0.125}$ itself exhibited excellent visible light catalytic performance as that the K value of the reaction rate reached 0.24, which was consistent with findings of Gnayem & Sasson (2013). For the β-Fe_2O_3-doped modified composites, the visible light catalytic degradation process of the RhB was significantly accelerated with the increase of Bi content in the composite. When the Bi content was gradually elevated

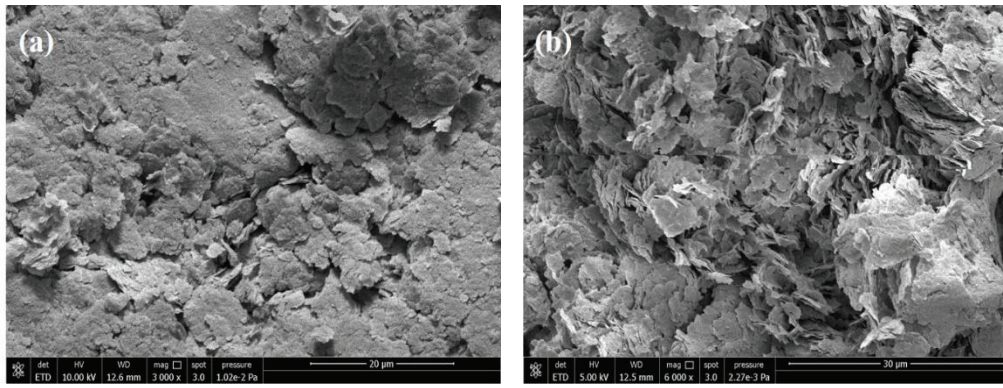

Fig. 2: SEM images of β-Fe_2O_3/$BiOCl_{0.875}Br_{0.125}$ with a magnification of (a) 3000, and (b) 6000.

to 30% (M4), the photocatalytic efficiency of the composite material had exceeded that of the pure $BiOCl_{0.875}Br_{0.125}$, with the highest K value of 0.26.

Mechanism of the enhanced photocatalytic activity: Based on the above experimental results and analysis, this experiment puts forward several interpretations about the enhanced photocatalytic performance of β-Fe_2O_3/$BiOCl_{0.875}Br_{0.125}$ on the degradation of RhB. First, semiconductor photocatalysis relies on the generation and separation of charge carriers, as well as the redox capability of semiconductors with different valence bands and conduction bands to improve the efficiency of interfacial charge transfer (Ge et al. 2011). It is known that β-Fe_2O_3 has a narrower bandgap (2.0~2.2) compared to $BiOCl_{0.875}Br_{0.125}$, and thus significantly enhances the response to visible light under light irradiation of λ>420 nm. The electrons on the β-Fe_2O_3 valence band are excited to reach a more potentially advantageous position to form a virtual conduction band, accordingly, these photogenerated electrons are more easily transferred to the conduction band of the relatively more positive $BiOCl_{0.875}Br_{0.125}$. In turn, it can effectively react with intermediates generated during the degradation process. This process can greatly reduce the recombination rate of photogenerated electrons and holes, thereby improving its photocatalytic performance. Second, photogenerated holes can react with OH^- in aqueous solution to form ·OH, while ·OH possesses strong oxidation capacity, which can oxidize organics quickly and efficiently. Third, the doping of β-Fe_2O_3 is beneficial to increase the specific surface area and pore volume of the composite catalyst, which is more favourable for the transfer of photogenerated electrons, holes and reactants to the reaction sites, thereby improving the photocatalytic performance of the catalyst (Martin et al. 2015).

CONCLUSION

BiOX-based composite photocatalyst has a good photocatalytic performance. The degradation rate of Rhodamine B solution reached 97.7% within 15 minutes under visible light irradiation, which was higher than most other photocatalysts.

The strategy of β-Fe_2O_3 doping BiOX shows great potential as that the introduction of β-Fe_2O_3 can significantly improve visible light response and reduce the recombination rate of the electron/hole pairs. Among the as-prepared β-Fe_2O_3/$BiOCl_{0.875}Br_{0.125}$ composite, the higher the content of Bi, the better the degradation effect was observed.

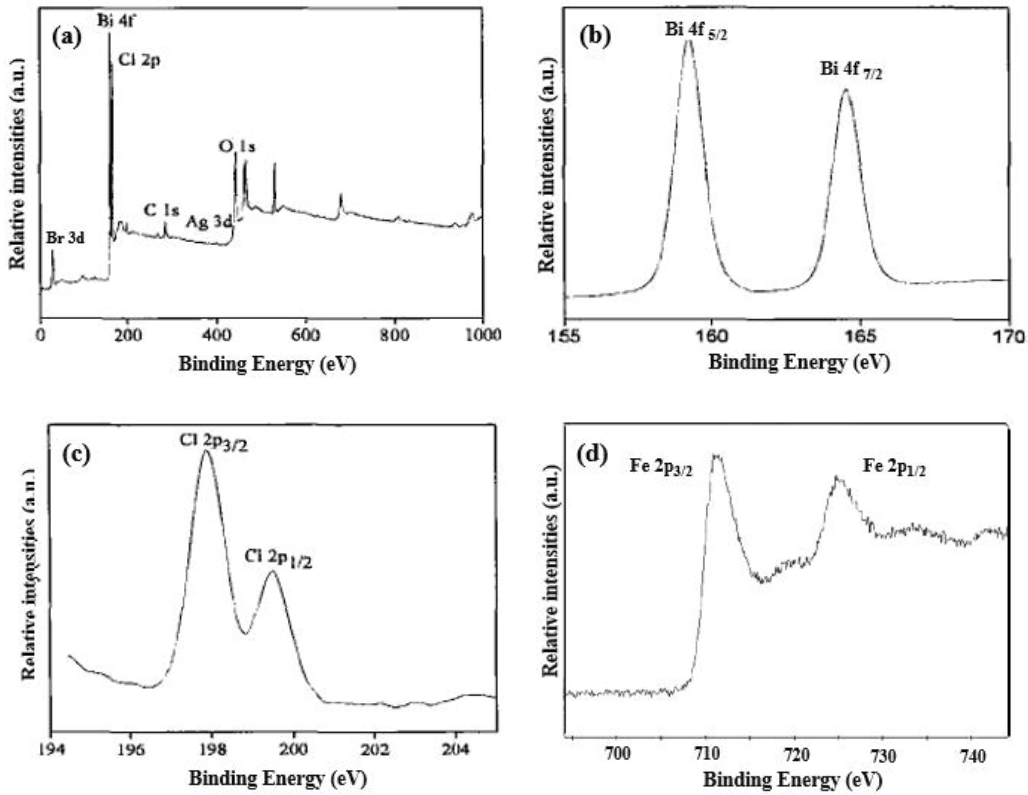

Fig. 3: XPS patterns of the composite β-Fe_2O_3/$BiOCl_{0.875}Br_{0.125}$: (a) survey, (b) Bi 4f, (c) Cl 2p, (d) Fe 2p.

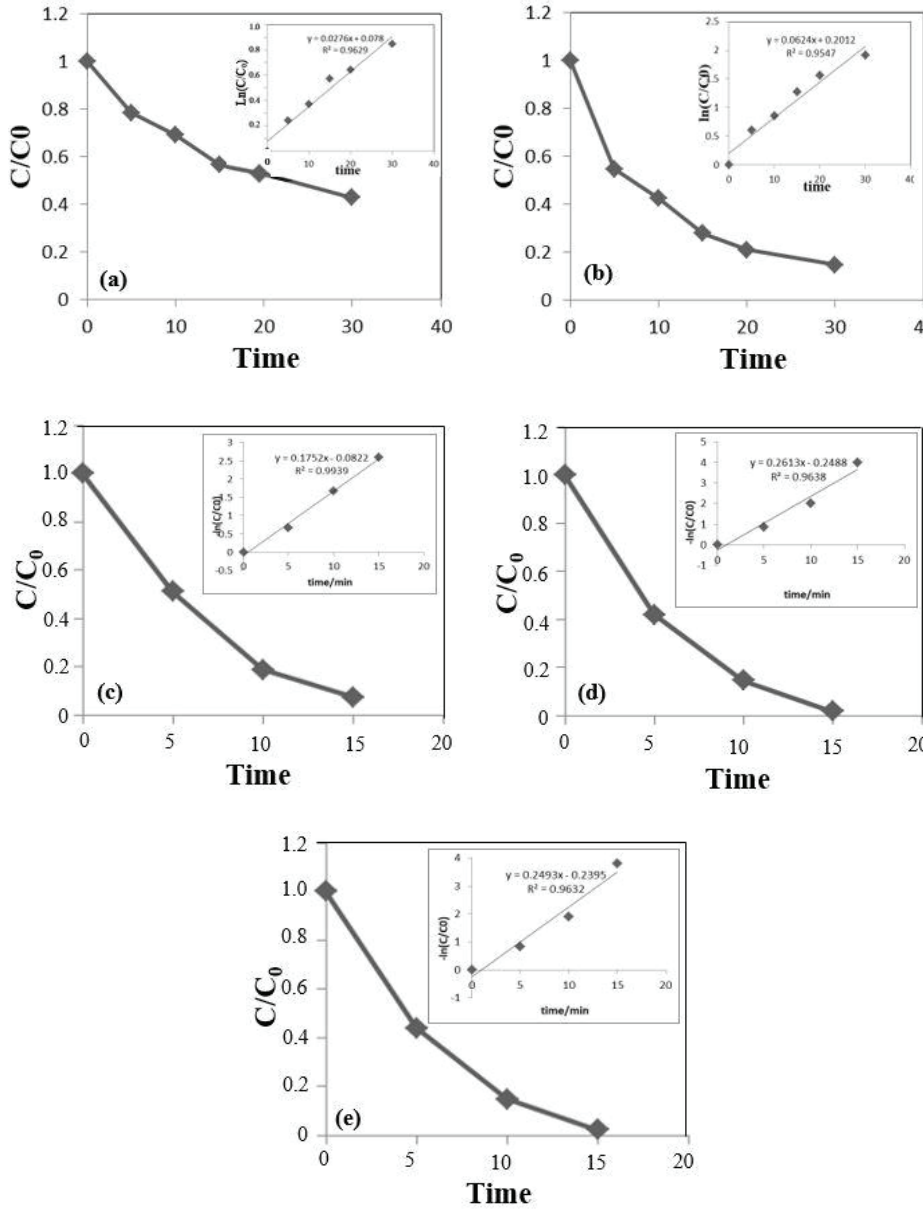

Fig. 4: Photocatalysis degradation efficiencies of RhB by various catalysts of (a) M1, (b) M2, (c) M3, (d) M4, (e) M0. The inset shows the quasi-first-order dynamic models corresponding to each process.

The modified β-Fe_2O_3/$BiOCl_{0.875}Br_{0.125}$ with Bi content of 30% can achieve a comparable and even better photocatalysis performance in comparison to an equal mass of pure phase $BiOCl_{0.875}Br_{0.125}$. Therefore, under the condition of ensuring catalytic efficiency, the material preparation cost can be greatly reduced.

ACKNOWLEDGEMENT

This work was financially supported by the Graduate Scientific Research and Innovation Foundation of Chongqing, China (Grant No. CYB18127).

REFERENCES

Amini, A., Kim, Y., Zhang, J., Boyer, T. and Zhang, Q. 2015. Environmental and economic sustainability of ion exchange drinking water treatment for organics removal. Journal of Cleaner Production, 104: 413-421.

Brázda, P., Kohout, J., Bezdička, P. and Kmječ, T. 2014. α-Fe_2O_3 versus β-Fe_2O_3: Controlling the phase of the transformation product of β-Fe_2O_3 in the Fe_2O_3/SiO_2 system. Crystal Growth & Design, 14(3): 1039-1046.

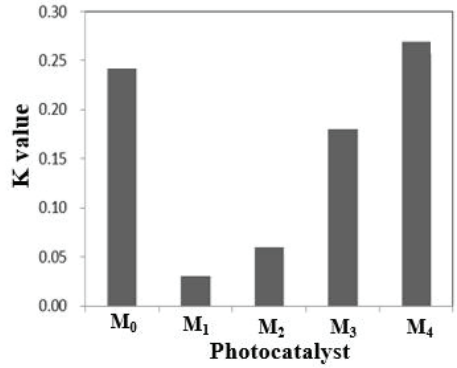

Fig. 5: Comparison of the K value of each photodegradation process.

Christoforidis, K. C., Montini, T., Bontempi, E., Zafeiratos, S., Jaén, J. J. D. and Fornasiero, P. 2016. Synthesis and photocatalytic application of visible-light active β-Fe_2O_3/g-C_3N_4 hybrid nanocomposites. Applied Catalysis B: Environmental, 187: 171-180.

Deng, H., Wang, J., Peng, Q., Wang, X. and Li, Y. 2005. Controlled hydrothermal synthesis of bismuth oxyhalide nanobelts and nanotubes. Chemistry-A European Journal, 11(22): 6519-6524.

Deng, Y. and Zhao, R. 2015. Advanced oxidation processes (AOPs) in wastewater treatment. Current Pollution Reports, 1(3): 167-176.

Elimelech, M. and Phillip, W.A. 2011. The future of seawater desalination: energy, technology, and the environment. Science, 333(6043): 712-717.

Ge, L., Han, C. and Liu, J. 2011. Novel visible light-induced g-C_3N_4/Bi_2Wo_6 composite photocatalysts for efficient degradation of methyl orange. Applied Catalysis B: Environmental, 108: 100-107.

Gnayem, H. and Sasson, Y. 2013. Hierarchical nanostructured 3D flowerlike $BiOClxBr_{1-x}$ semiconductors with exceptional visible light photocatalytic activity. ACS Catalysis, 3(2): 186-191.

Hasan, Z. and Jhung, S. H. 2015. Removal of hazardous organics from water using metal-organic frameworks (MOFs): plausible mechanisms for selective adsorptions. Journal of Hazardous Materials, 283: 329-339.

Hoffmann, M.R., Martin, S.T., Choi, W. and Bahnemann, D.W. 1995. Environmental applications of semiconductor photocatalysis. Chemical Reviews, 95(1): 69-96.

Jaiswal, R., Patel, N., Dashora, A., Fernandes, R., Yadav, M., Edla, R., Varma, R. S., Kothari, D. C., Ahuja, B. L. and Miotello, A. 2016. Efficient Co-B-co-doped TiO_2 photocatalyst for degradation of organic water pollutant under visible light. Applied Catalysis B: Environmental, 183: 242-253.

Lee, K. M., Lai, C. W., Ngai, K. S. and Juan, J. C. 2016. Recent developments of zinc oxide based photocatalyst in water treatment technology: a review. Water Research, 88: 428-448.

Li, J., Yu, Y. and Zhang, L. 2014. Bismuth oxyhalide nanomaterials: layered structures meet photocatalysis. Nanoscale, 6(15): 8473-8488.

Martin, D. J., Liu, G., Moniz, S. J., Bi, Y., Beale, A. M., Ye, J. and Tang, J. 2015. Efficient visible driven photocatalyst, silver phosphate: performance, understanding and perspective. Chemical Society Reviews, 44(21): 7808-7828.

Masih, D., Ma, Y. and Rohani, S. 2017. Graphitic C_3N_4 based noble-metal-free photocatalyst systems: A review. Applied Catalysis B: Environmental, 206: 556-588.

Mohamed, A., El-Sayed, R., Osman, T. A., Toprak, M. S., Muhammed, M. and Uheida, A. 2016. Composite nanofibers for highly efficient photocatalytic degradation of organic dyes from contaminated water. Environmental Research, 145: 18-25.

Omenn, G.S. 2006. Grand challenges and great opportunities in science, technology, and public policy. Science, 314(5806): 1696-1704.

Ren, K. X., Liu, J., Liang, J., Zhang, K., Zheng, X., Luo, H. D., Huang, Y. B., Liu, P. J. and Yu, X. 2013. Synthesis of the bismuth oxyhalide solid solutions with tunable band gap and photocatalytic activities. Dalton Transactions, 42(26): 9706-9712.

Ribeiro, A. R., Nunes, O. C., Pereira, M. F. and Silva, A. M. 2015. An overview on the advanced oxidation processes applied for the treatment of water pollutants defined in the recently launched Directive 2013/39/EU. Environment International, 75: 33-51.

Xiao, X., Liu, C., Hu, R., Zuo, X., Nan, J., Li, L. and Wang, L. 2012. Oxygen-rich bismuth oxyhalides: generalized one-pot synthesis, band structures and visible-light photocatalytic properties. Journal of Materials Chemistry, 22(43): 22840-22843.

Zhang, L. P., Liu, Z., Faraj, Y., Zhao, Y., Zhuang, R., Xie, R., Ju, X. J., Wang, W. and Chu, L. Y. 2019. High-flux efficient catalytic membranes incorporated with iron-based Fenton-like catalysts for degradation of organic pollutants. Journal of Membrane Science, 573: 493-503.